Physica Scripta. Vol. T110, 141–143, 2004

Doubly Excited States in Helium Close to the Double Ionization Threshold: Angular and Energy Resolved Partial Cross Sections

A. Czasch[1,*], M. Schöffler[1], T. Jahnke[1], S. Schössler[1], M. Hattass[1], Th. Weber[1], M. Weckenbrock[1], J. Titze[1], C. Wimmer[1], A. Staudte[1], S. Kammer[1], S. Voss[1], R. Dörner[1], H. Schmidt-Böcking[1], J. M. Rost[2], T. Schneider[2] and C. Liu[3]

[1] Institut für Kernphysik, Universität Frankfurt, Germany
[2] Max–Planck-Institut für Physik komplexer Systeme, Dresden, Germany
[3] Department of Physics, Cardwell Hall, Kansas State University, Manhattan, Kansas, USA

Received September 5, 2003; accepted January 16, 2004

PACS ref: 32.80.Fb

Abstract

This is a report about a novel experiment on double excitation of Helium by absorption of synchrotron radiation close to the double ionization threshold at 79 eV. Partial cross-sections for single-ionization from 78.15 eV up to 78,9 eV (photon energy) with an energy resolution of 3 meV have been measured. The technique described in this article allows for an angular and energy resolved measurement of low energy electrons with a high detection efficiency due to an angular acceptance of 4π solid angle.

1. Introduction

Double highly excited states of Helium have been subject of many theoretical and experimental works in the recent decades [1–18]. These are ideal candidates for the search for quantum chaos manifested in Ericson fluctuations in an un-perturbed quantum system. Double highly excited states can be investigated by direct detection of metastable states [20,22] or by analyzing different decay paths with methods of photon [19–22] or electron spectroscopy. The latter one will be discussed in this article. In principal there are two interfering undistinguishable pathways leading to the same final states:

via a doubly excited state

$$\gamma(< 79\,\mathrm{eV}) + \mathrm{He} \rightarrow \mathrm{He}^{**} \rightarrow \mathrm{He}^{+}(n) + \mathrm{e}^{-}$$

or by direct ionization

$$\gamma(< 79\,\mathrm{eV}) + \mathrm{He} \rightarrow \mathrm{He}^{+}(n) + \mathrm{e}^{-}.$$

Partial cross sections $\sigma(n)$ and angular distributions are known up to the threshold for $n = 5$ of the residual He^+-ion (n being the principal quantum number) [2]. For several years there was no significant experimental progress in this field. Partial cross sections above $n = 5$ are very low and traditional techniques reached their limits as the measurements were too time-consuming. In general spectroscopy of low energy electrons with traditional techniques is a very difficult task. On the other hand recent measurements of the total cross section have reached the $n = 11$ threshold [4,12–16]. The authors of these works claim to see first evidence for quantum chaos in Helium in this region [4]. Therefore we were very interested in measuring partial cross-sections and angular distributions in this region. In order to overcome the problems of low partial cross-sections and low energy electrons we based our experimental setup on the COLTRIMS-technique [25]. The primary advantage of this three-dimensional imaging technique is a high detection efficiency due to an angular acceptance of 4π solid angle around the target zone. This technique is known to be well suited for low energy electron detection [24], however high resolution in combination with accurate linearity in all three spatial dimensions for electrons below 500 meV remained an interesting challenge for the present application. However, all these problems, including the distortion of electron trajectories by the earth's magnetic field, turned out to be easy to handle and the first two beamtimes at the synchrotrons HASYLAB at DESY (BW3) in Hamburg and BESSYII in Berlin (U125/1PGM) were very successful.

2. The technique

In the following paragraphs a short overview of the technique will be given. The details will be described in the subsequent sections of this article.

A narrow supersonic Helium gas jet was intersected by the pulsed photon beam produced by the synchrotron radiation facility BESSY II. Thus the size of the reaction zone was given by the width of the photon beam (150 μm × 30 μm) and the diameter of the gas jet (3 mm). The size of this zone does not affect the resolution of the apparatus but is merely crucial for the suppression of background. The negative effects of this uncertainty in the starting position can be eliminated by using the information about the He^+-ion, which was measured in coincidence. The density of the gas target was approximately $10^{12}\,\mathrm{cm}^{-2}$.

The emission of the electrons can occur in any direction. In order to detect all electrons with one detector a weak electrostatic guiding-field (2 V/cm) was applied homogenously inside the spectrometer. The same field drove the He^+-ions towards a second detector mounted at the opposite end of the spectrometer. Both particles were detected in coincidence. The coincident measurement of position and time-of-flight of electron and ion provided an excellent background suppression (see Fig. 3). The final positions on the detectors and the flight-times were recorded in list-mode. This information is sufficient for

* e-mail: czasch@hsb.uni-frankfurt.de

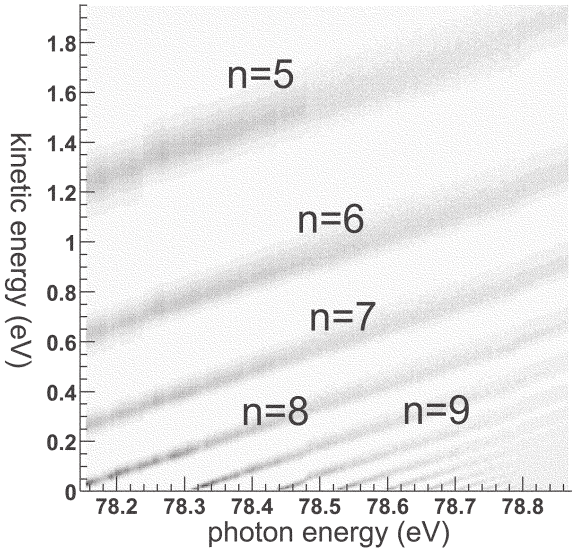

Fig. 1. Single-ionization of helium close to the double-ionization threshold at 79 eV. Horizontal axis: photon energy (scanned with 3 meV resolution). Vertical axis: electron energy. The grey scale shows the count rate in arbitrary units. With increasing photon energy more final states of the residual $He^+(n)$-ion can be populated. Partial cross-sections $\sigma(n, \gamma)$ and angular distributions $\beta(n, \gamma)$ have been measured.

the calculation of the initial kinetic energy and direction of emission of the electrons.

3. The detectors

Two detectors were used—one for the detection of electrons and one for the He^+-ions. The detectors are composed of a stack of micro-channel-plates and a delay-line anode for two-dimensional position readout [23]. The active area is 80 mm in diameter. The time of arrival of a particle and the final position can be measured with a resolution of 0.4 ns and 0.3 mm respectively (FWHM). One advantage of the delay-line technique is multi-hit-capability. Although not crucial for this experiment regarding its basic requirements the multi-hit capability yields a major advantage for the offline data-analysis: if multiple electrons were detected simultaneously it is possible to identify the one which corresponds to the He^+-ion (via momentum conservation) and separate it from stray electrons.

4. The spectrometer

As described above it was necessary to apply a weak and highly homogenous electrostatic field across the reaction zone in order to guide the particles towards the two-dimensional detectors. A linear combination of rings made of copper served for this purpose. The rings were connected with a chain of resistors. Thus applying a potential difference across this structure generated a homogenous field inside the spectrometer. The spacing between the rings had to be small enough (5 mm) to avoid penetration of fringe fields from outside of the spectrometer (Fig. 2).

The exact dimensions of the spectrometer were optimized by Monte Carlo simulations. The resulting dimensions represent a compromise between several competing constraints. On the one hand a weak electrostatic field is favorable. This leads to a maximum spread for the times-

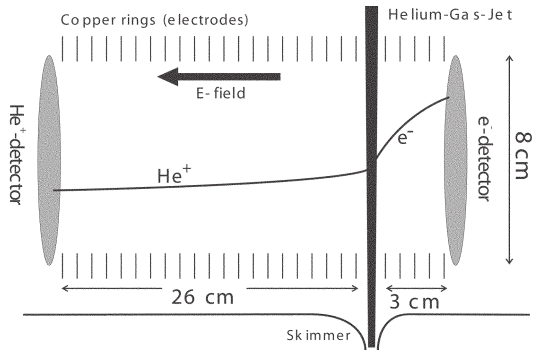

Fig. 2. Sketch of the spectrometer. The photon-beam (not displayed) intersects the gas-target. The emitted particles are separated in a weak

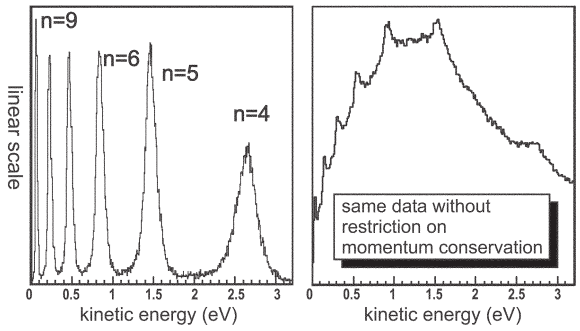

Fig. 3. An example for typical spectra of kinetic energies of the emitted electrons. The two pictures demonstrate the importance of background suppression. The different widths of the peaks are discussed in the main text.

of-flight of the particles. On the other hand if the field is too weak some electrons might not be collected on the detector. The optimal configuration was determined to be 2 V/cm with a distance between target and electron detector of 3 cm. Due to momentum conservation the much heavier He^+-ion receives less energy. Therefore the distance between target and He^+-detector had to be as large as possible to ensure a sufficient spread across the detector. In our case this length was limited to 26 cm by the inner bounds of the vacuum chamber. Time-focusing of the flight-times was not necessary. Since both particles were detected in coincidence and due to momentum conservation the uncertainty in the starting position can be eliminated analytically.

5. Background suppression

A doubly excited state can decay into different final states which can be identified by the principal quantum number n of the residual He^+-ion. $He^+(n = 1)$ is the dominant process—being roughly three magnitudes more intense than channels above $n = 8$. This primary process produces electrons with a kinetic energy of more than 50 eV (at a photon energy of 78 ± 1 eV). These electrons are well separated from slower ones in time-of-flight, which allows for a simple but efficient suppression during the measurement. A far more serious problem is caused by secondary electrons that are produced inside the spectrometer when a fast electron hits a surface. These secondary electrons produce signals on the detector that cannot be distinguished online from real slow electrons coming from the target zone. However later during the off-line analysis it is possible to sort out these events by checking momentum

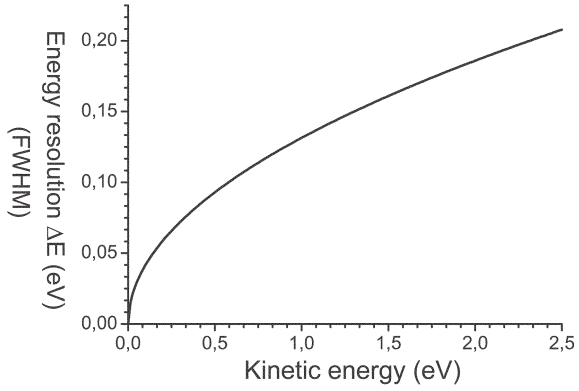

Fig. 4. Since the resolution in momentum space is constant ($17.5 \cdot 10^{-3}$ a.u. FWHM) the resolution in energy is better at small kinetic energies ($\Delta E \sim E^{1/2}$).

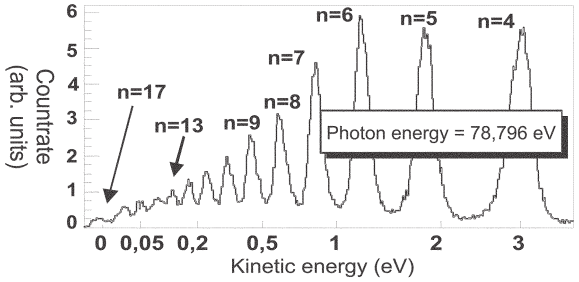

Fig. 5. Discrete levels of kinetic energies correspond to different final states of $He^+(n)$. The peaks corresponding to $n = 5$ and $n = 4$ are too low due to a decreased detection efficiency for electrons with kinetic energies of more than 1.7 eV.

conservation between the electron and the He^+-ion. This condition reduces the amount of background tremendously (see Fig. 3 below).

6. Data analysis

The data were stored in list-mode. This means that the final positions and the flight-times of the particles were recorded individually for every single event. Thus the entire beamtime can be replayed in fast motion in the offline analysis. The initial kinetic energy and direction of emission can be easily derived from the recorded positions and flight-times if there is no magnetic field present. However since we decided not to shield our system against the earth magnetic field (which was not oriented parallel to the electric field) the formalism became more complex. In this case the trajectories were no longer parabolic but had the shape of cycloids. Still the resulting differential equations can be solved analytically. This would not be possible if a more complicated field-configuration had been used, e.g., for time-focusing purposes. It was not necessary to measure the magnetic field *in situ*—instead the field-components can be extracted from the data itself. This is possible because the levels of kinetic energies are discrete and because certain geometrical symmetries must be preserved, e.g., the angular distribution of the electrons must be symmetrical to the plane perpendicular to the polarization-vector of the light. These constraints are sufficient to reconstruct the three components of the magnetic field.

7. Results and summary

During two beamtimes a large photon energy region from $E_\gamma = 78,15\,\text{eV}$ up to $E_\gamma = 78,9\,\text{eV}$ with a step-size and energy-resolution of 3 meV (FWHM) has been scanned (see Fig. 1). A total data-acquisition time of 9 days was sufficient for the entire scan. Different final states of $He^+(n)$ from $n = 5$ to $n = 11$ are clearly separated and levels up to $n = 17$ can be identified (Fig. 5). In Fig. 3 it is clearly visible that the energy resolution of the apparatus is not a constant but a function of the kinetic energy itself ($\Delta E \sim \sqrt{E}$, see Fig. 4). This is due to the fact that the design of the spectrometer leads to a constant resolution in momentum space and not in energy space. This is an important fact for the experiment because it allows for the separation of highly excited levels, which would be difficult to identify otherwise (Fig. 5). Extraction of partial cross-sections $\sigma(\text{n}, \gamma)$ and angular distributions $\beta(\text{n}, \gamma)$ and comparison to theoretical calculations is currently under way.

References

1. Madden and Codling, Phys. Rev. Lett. **10**, 516 (1963).
2. Menzel, A., Frigo, Whitfield and Caldwell, Phys. Rev. A **54**, 2080 (1996) and Phys. Rev. Lett. **75**, 1479 (1995)
3. Rost, Liu, C. and Schneider, Phys. Rev. A **65**, (2002).
4. Püttner *et al.*, Phys. Rev. Lett. **86**, 3747 (2001).
5. Greene, Phys. Rev. Lett. **44**, 869 (1980).
6. Rost, Schulz, Domke and Kaindl, J. Phys. B: At. Mol. Phys. **30**, 4663 (1997).
7. Rost, J. Phys. B: At. Mol. Opt. Phys. **27**, 5923 (1994).
8. Leopold und I. C. Percival, J. Phys. B: At. Mol. Phys. **13**, 1037 (1980).
9. Rost and Briggs, J. Phys. B: At. Mol. Phys. **24**, 4293 (1991).
10. Rev. Mod. Phys. **72**, (2000).
11. Gutzwiller, M. C. "Chaos in Classical and Quantum Mechanics" (Springer, New York, 1990).
12. Wintgen and Delande, J. Phys. B: At. Mol. Opt. Phys. **26**, L399 (1993).
13. Püttner *et al.*, J. Electr. Spec. Rel. Phen. **101–103**, 27 (1999).
14. Domke, Schulz, Remmers and Kaindl, Phys. Rev. A **53**, 1424 (1996).
15. Domke, Schulz, Remmers, Gutiérrez and Kaindl, Phys. Rev. A **51**, R4309 (1995).
16. Domke *et al.*, Phys. Rev. Lett. **66**, 1306 (1991).
17. Lin, C. D. Phys. Rev. Lett. **51**, 1348 (1983) and Phys. Rev. A **29**, 1019 (1984).
18. Herrick, D. R. und Sinanolu, O., Phys. Rev. A **11**, 97 (1975).
19. Gorczyca *et al.*, Phys. Rev. Lett. **85**, 1202 (2000).
20. Penent *et al.*, Phys. Rev. Lett. **86**, 2758 (2001).
21. Rubensson *et al.*, Phys. Rev. Lett. **83**, 947 (1999).
22. Odling-Smee, M. K., Sokell, E. and Hammond, P., Phys. Rev. Lett. **84**, 2598 (2000).
23. Jagutzki, O. *et al.*, "Imaging Spectroscopy IV", Michael R. Descour, Sylvia Shen, SPIE Proceedings Vol. 3438, pp. 322 (1998) (and www.roentdek.com).
24. Moshammer, R., Ullrich, J., Unverzagt, M., Schmidt, W., Phys. Rev. Lett. **73**, 3371 (1994).
25. Dörner, R. *et al.*, Phys. Rep. 330 (2000).

